

INVESTIGATION OF TEMPERATURE STATE OF COPPER PLATES IN THE WELD ZONE AT FRICTION STIR WELDING

M.A. Polieshchuk, A.V. Shevtsov, I.V. Dotsenko,

V.M. Teplyuk, O.V. Kolisnichenko and L.M. Malakhova

E.O. Paton Electric Welding Institute of the NAS of Ukraine

11 Kazymyr Malevych Str., 03150, Kyiv, Ukraine. E-mail: office@paton.kiev.ua

Chromel-alumel thermocouples were used to study the temperature state of 10 mm copper plates at simulation of the process of friction stir welding. Thermocouples were welded on in blind holes located along the line of welding tool movement that allowed recording the copper temperature at the moment of weld formation in different welding modes. In the studied range of variation of process parameters, the metal temperature is mainly influenced by the area of interaction of the welding tool working surface with the plate, while the speed of tool rotation has a minor effect. At the moment of weld formation the metal temperature varied from 528 up to 980 °C in different modes. 13 Ref., 3 Tables, 3 Figures.

Keywords: friction stir welding, copper plates, thermocouples, welds, formation temperature

Relevance and objective of the work. A new technology of joining metal materials – friction stir welding (FSW), patented by The Welding Institute (Great Britain) in 1991, has been developed recently [1]. This technology is realized, using a special rotating tool (Figure 1), which is immersed into the butt of the parts being welded, and moves along it. The working part (1) of this tool has a central rod — pin (2), designed for heating by friction the edges being welded. Located above the pin is the shoulder (3), which forms the weld. The tool working part is fastened in mandrel (4), which is inserted into the welding machine spindle.

Heating of edges being welded is performed due to the tool friction against their surfaces. The heat created by friction and deformation, heats the metals being joined to a plastic state, while the linear movement of the rotating tool, leads to stirring of the plasticized metal volumes, resulting in joint formation. The shape, dimensions and hardness of the material of the tool working part are determined by the welded material grade and its thickness.

FSW technology differs from all kinds of fusion welding by absence of the liquid metal phase in weld formation zone, the solidification of which may lead to defects in the form of shrinkage and liquation cracks and porosity. Thus, this technology allows obtaining a better quality weld, and also joining dissimilar metals and alloys, which cannot be welded by other welding methods. FSW technology was first created for welding relatively low-melting materials, mainly alumin-

ium alloys [2]. Work on FSW application for copper [3] and steels [4, 5] began somewhat later.

When developing the FSW technology, it is important to know the temperature level in the zone of weld formation. This information allows determining the optimal process parameters of welding, namely frequency and speed of the tool linear movement, and also assessing the resistance of the material of its working part. Unfortunately, the main scope of data on metal temperature in the zone of weld formation is assessed by the results of measurement of metal temperature in the zone located in immediate vicinity of the weld.

The maximum values of temperature at FSW of some metals, published by different authors, are summarized in Table 1. One can see from the Table that

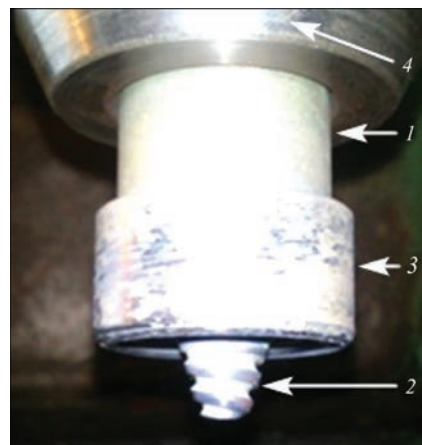


Figure 1. Welding tool for FSW (for designations see the text)

M.A. Polieshchuk — <https://orcid.org/0000-0002-5992-4641>, A.V. Shevtsov — <https://orcid.org/0000-0001-9599-4842>,
I.V. Dotsenko — <https://orcid.org/0000-0002-1040-0409>, V.M. Teplyuk — <https://orcid.org/0000-0002-0463-0689>,
O.V. Kolisnichenko — <https://orcid.org/0000-0003-4507-9050>, L.M. Malakhova — <https://orcid.org/0000-0003-1388-6536>

© M.A. Polieshchuk, A.V. Shevtsov, I.V. Dotsenko, V.M. Teplyuk, O.V. Kolisnichenko and L.M. Malakhova, 2021

Table 1. Metal temperature in the vicinity of welds at FSW

Number	Alloy	Measurement location	Temperature, °C	Ref.
1	AA6061-T6	On weld surface and in the center	425	[6]
2	AA7075-T651	~0.6 mm (0.02") below the top that is adjacent to the stirring zone	475	[6]
3	AA6061-T6	–	310	[6]
4	AA1050	Close to the lower limit of stirring zone	310	[6]
5	AISI-1018	Interface of the shoulder and processed item	990	[6]
6	AA2195-T8	Region adjacent to pin edge	450	[6]
7	AZ-31	In the HAZ	360	[6]
8	Pure copper C1 1000	Same	530	[7]
9	Pure copper Cu-OF	Region adjacent to pin edge	850	[3]
10	Al alloy 1561	On the boundary of weld metal with base metal	475	[8]

all the given in it temperature values are below the solidus temperature of the respective alloys.

PWI is working to develop FSW technologies for different metals [9, 10]. Particular attention is given to problems of welding copper and its alloys by FSW method, as these materials are widely used in metallurgical engineering for manufacture of different types of water-cooling crucibles [11]. In addition, the structures of welds from dissimilar metals with different solubility of elements in the solid phase were studied for the case of protective layer deposition on copper bases [12].

Materials and procedure of investigations. At development of optimal process parameters of FSW of copper detailed studies of the temperature state of copper plates in the zone of weld formation were conducted. Temperature measurement and recording was performed at simulation of FSW process on rectangular plates from M1 copper 10 mm thick with application of chromel-alumel thermocouples, installed in blind holes made in the plate body. The holes were made to have such depth that the distance from the thermocouple junction to the pin edge passing above it, was not more than 1 mm. Thermocouple junctions were fastened to the hole bottoms by capacitor-discharge welding, and their cold ends were connected to signal amplifier. After amplification the thermo-EMF signal was saved in the computer through analog-digital amplifier NI USB-6009, National Instrument. The sampling rate was 2 s^{-1} . Labview development environment was used for organizing the recording and visualization of temperature change during the entire technological process. This measurement schematic allowed simultaneously recording the readings of four thermocouples with 10 % calculation error. In order to record the temperature, two thermocouples were located along the line of welding tool movement, thermocouple No.1 was placed in the point of pin immersion into the plate body, while thermocouple No.2 was located at 40 mm distance from it. Testing was preceded by calibration of thermocouples, fastened in the plate body at 0 and 100 °C. Temperature, recorded by the thermocouples, was compared with the read-

ings of control thermometer of TR-101 grade with division value of 0.1 °C. The error of metal temperature measurement did not exceed 4 %.

Two welding tools with the same shoulders of 34 mm diameter and pins of different dimensions were used during investigations. One tool had a larger pin with 16 mm diameter of the base, 5.5 mm tip diameter and 8.5 mm height. The other one had a pin of smaller dimensions of 10, 3.5 and 6.5 mm, respectively. The axis of weld tool rotation was deviated from the vertical by 1.5° to the side opposite to the direction of horizontal movement.

Two groups of experiments were conducted. In the first group, just the pin was immersed into the plate body, while the shoulder was at 0.1 mm distance from its surface. In the second group of experiments a standard FSW process was simulated.

Investigation results and discussion. In the first group, the process started from the pin immersion into the plate surface above the point of location of thermocouple No.1. Before that 0.1 mm foil was pasted to the plate surface in this site. At the moment the shoulder lower edge touched the foil, the tool immersion was stopped, and its horizontal movement was began in the direction of thermocouple No.2. During investigations temporary cutting off was performed in the graphs of thermocouple readings: the first at the moment of the pin edge touching the plate surface, the second — at the moment of the start of the tool horizontal movement, and the third — at the moment of the pin passing over the second thermocouple. Table 2 gives the values of FSW process mode parameters: welding tool rotation frequency (RF), its horizontal movement speed (MS), as well as the specified shape of welding tool working parts with a large (LP) and small (SP) pins. In addition, the Table gives the maximum temperature values, recorded in these modes by the first thermocouple (t_1) and second thermocouple (t_2).

Two curves of temperature change in the studied points of the copper plates were derived in each FSW mode. Figure 2 shows examples of temperature curves, obtained in the first (a) and second (b) process modes of

FSW (see Table 2). At other modes, graphs of a similar shape were obtained that differ by the values of maximum temperature recorded by the thermocouples.

In the point of immersion of the welding tool into the plate body, copper temperature starts increasing right after the pin edge touches its surface (cut-off 1). As the pin goes down, the temperature rises and reaches its maximum at the moment the introduction process is over. After the start of horizontal movement of the working tool (cut-off point 2) the temperature in this site decreases, because of removal of the heat evolution source from the measurement point. Temperature curves, recorded by the first thermocouples, show that at the moment of the welding tool immersion, the heat evolves predominantly due to friction. This is confirmed by analysis of maximum temperature values in these sites at FSW in different modes (see Table 2). Indeed, the maximum temperature value mainly depends on the area of friction surface, while the influence of the frequency of welding tool rotation is insignificant.

The graphs of the change of copper temperature, fixed by thermocouples No.2, show that the start of temperature increase in these points lags behind the readings of the first thermocouple, as the heat is transferred to them due to heat conductivity. The delay time is determined by the velocity of temperature propagation in copper. After the start of horizontal movement of the welding tool, the power of the heat evolution source rises owing to additional heat from plastic deformation of metal near the pin. In the graphs, these temperature changes are reflected in the form of increase of the angle of inclination to the horizontal axis of temperature curves in thermocouples No.2. When the welding tool moves closer to the locations of the other thermocouples, further increase of the rate of temperature rise takes place. The magnitude of metal temperature reaches the maximum values at the moment of the pin passing over thermocouple No.2 (cut-off 3).

Analysis of temperature values, given in Table 2, shows that the plate temperature in the locations of

Table 2. FSW mode parameters in the first group of experiments

Mode number	Pin shape	RF, rpm	MS, mm/min	$t_1, ^\circ\text{C}$	$t_2, ^\circ$
1	SP	800	40	216	312
2	LP	800	40	438	557
3	LP	800	50	441	559
4	LP	1000	40	456	571

thermocouples No.2 is approximately $100\text{ }^\circ\text{C}$ higher than in the points of the pin immersion. It is obvious that temperature increase in the location of thermocouple No.2 is the result of additional heat evolution, associated with plastic deformation of the plate material. This temperature essentially depends on the pin dimensions, i.e. on the area of interaction of the welding tool working part with the plate material. Maximum temperature was recorded by us at simulation of FSW with 1000 rpm frequency of the tool rotation. No influence of the speed of horizontal movement of the welding tool working part was found in the studied range.

Analysis of temperature curves, given in Figure 2 suggested that two variants of heating the edges of the products being welded are possible at FSW of metal materials with high heat conductivity. At linear movement speeds smaller than the linear velocity of temperature propagation in the welded product material, metal preheating occurs ahead of the tool front, so that additional heat evolution from the tool operation takes place in more heated regions. Metal temperature at the moment of weld formation will rise with their length. If the welding tool speed is higher than the velocity of temperature propagation, metal preheating ahead of the rotating front is absent, and increase of weld formation temperature will not occur along the division line.

The velocity of temperature propagation in metals is determined by the thermal diffusivity, which is numerically equal to the ratio of the coefficient of heat conductivity to specific heat, and has the dimension of m^2/s . This coefficient should be regarded as the surface area, ahead of the front of which increase of the metal

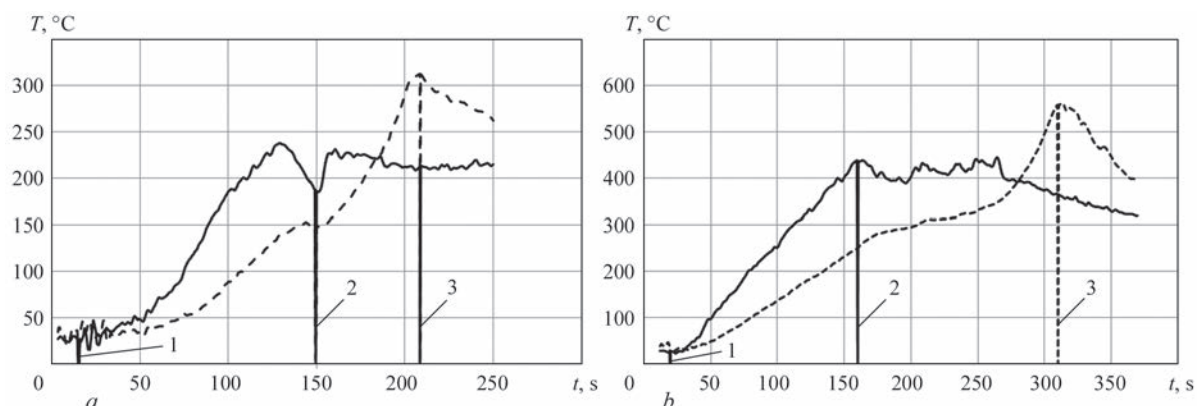


Figure 2. Graphs of the change of copper plate temperature during FSW: *a* — 800/40 SP; *b* — 800/40 LP (solid line shows temperature changes in the points of pin immersion; intermittent — in the location of the second thermocouple); 1, 2, 3 — temporary cut-offs (for description see the text)

Table 3. FSW mode parameters in the second experimental series

Mode parameters	Mode number									
	1	2	3	4	5	6	7	8	9	10
RF, rpm	800	800	800	1000	1000	1000	800	800	1000	1000
MS, mm/min	40	40	40	50	50	50	40	40	40	50
TD, mm	0.36	0.4	0.6	0.2	0.4	0.6	0.3	0.5	0.2	0.35
IA, mm ²	180.88	194.96	280.77	130.88	194.96	280.77	160.13	235.11	130.88	177.55
t_1 , °C	–	–	–	–	–	–	644	588	428	660
t_2 , °C	700	710	900	530	780	980	670	695	528	715

initial temperature occurs in a unit of time. Theoretically, for a semi-closed body such a surface will be a widening half-sphere, in the center of which a point heat source is acting. For plates, such a surface will be the upper spherical segment of the half-sphere, the height of which is equal to the plate thickness. The radius of the half-sphere that expanded per a unit of time, can be regarded as the linear velocity of temperature propagation over the surface of the body or plates.

For different copper grades, the thermal diffusivity is in the range of 111.0–115.0 mm²/s [13]. Here, the theoretical linear velocity of temperature propagation for copper plates 10 mm thick is equal to 108 mm/min on average. However, the real linear velocity of temperature propagation in the copper plates at FSW can be smaller than the theoretical value, as the working surface of the welding tool does not create a point heat source, while the plate proper is lying on a metal substrate with another thermal diffusivity value that makes corrections in the total surface area of the half-sphere spherical segment.

The real velocity of temperature propagation in the copper plates 10 mm thick in different FSW modes was assessed by us experimentally. For this purpose, the lapse of time between the moments of the beginning of metal temperature rise in the points of location of thermocouples No.1 and No.2 was determined in

the temperature curves (Figure 2). These data were the basis for determination of the average velocity of temperature propagation for all FSW modes. This velocity was equal to approximately 100 mm/min. Thus, the speed of horizontal movement of the welding tool of 100 mm/min, can be optimal to ensure a constant temperature in the joint zone along the entire weld length for the copper plates 8 to 12 mm thick (although this assumption requires additional experimental verification). In the second group of experiments, simulation of the standard FSW process with different frequency of rotation and speed of welding tool movement and different area of interaction of its working part with the plate, was performed. This area was determined by the depth of the trace left by the shoulder on the plate surface after welding, using the tool drawing in SOLIDWORK design program.

Thus, considering the errors, arising at measurement of all the parameters, which determine FSW modes (rotation frequency, movement speed, trace depth, accuracy of placing the thermocouples in the plate body), the overall computed error of temperature measurements, when performing the second group of experiments, was equal to 20 %. Specific parameters of the studied FSW modes are given in Table 3, which additionally shows the shoulder trace depth (TD) and area of the tool interaction with the plate (IA).

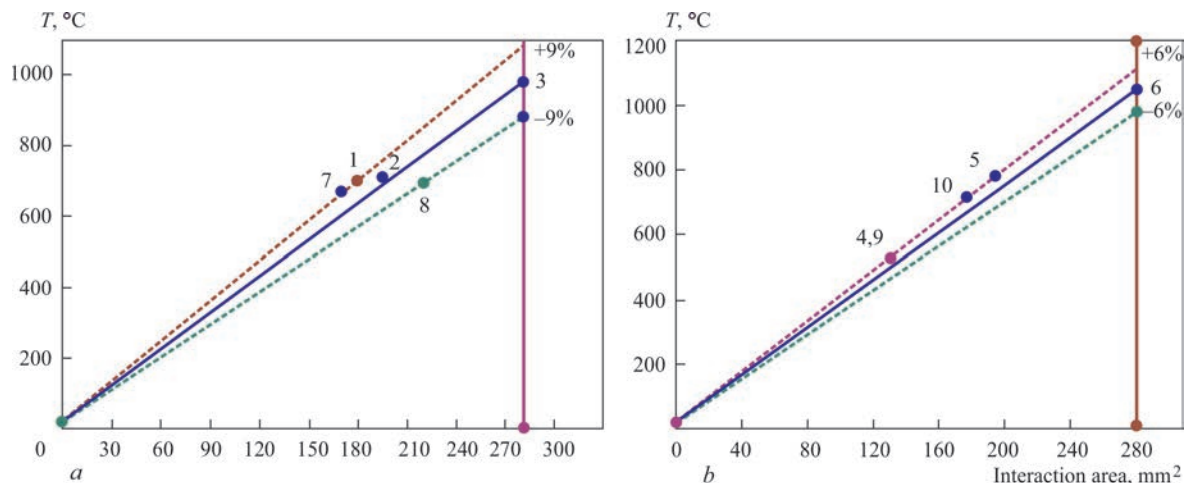


Figure 3. Dependence of copper temperature on interaction area: *a* — RF 800 rpm; *b* — 1000 (point numbers correspond to FSW modes, Table 3)

The shape of temperature curves, derived in all FSW modes in the second series of experiments, is similar to those given in Figure 2. An essential point of difference is the value of metal temperature. This temperature is lower than that of copper melting in all FSW modes, given in the table. At metallographic studies no cast structures were found in the weld cross-sections even in FSW modes, at which the metal temperature reached 900 and 980 °C. Thus, the results of experimental studies convincingly confirm that at FSW of copper the liquid metal phase is absent at the moment of weld formation.

In the studied range of process parameters variation at FSW, the metal temperature at the moment of weld formation mainly depends on the area of welding tool interaction with the plate body.

Figure 3 shows the graphs of these dependencies at welding tool rotation frequencies of 1000 (a) and 800 rpm (b). These graphs are plotted by generalization of maximum values of metal temperature at the respective rotation frequency (Table 3). The error of plotting the graphs was smaller than the computed error of temperature measurement in the conducted experiments. One can see from the graphs that the metal temperature changes significantly at minimum change of the depth of welding tool immersion into the plate body. This fact accounts for a wide range of experimental values of metal temperature at the moment of weld formation at FSW of specific metal materials given in publications. In the studied range, the frequency of welding tool rotation has a minor influence on metal temperature at weld formation. No influence of the change in the speed of welding tool movement from 40 to 50 mm/min was found.

The next paper will give the results of studying the metal temperature at the moment of weld formation in a wide range of change of rotation frequency and speed of welding tool horizontal movement, as well as distribution of temperature values in the weld cross-section.

Conclusions

1. At FSW of copper, the temperature of weld formation is mainly determined by the area of interaction of the working part of the welding tool with the plate body. In the studied range at minimal interaction area, the copper temperature in the site of weld formation is equal to 528 °C, and at maximum temperature it reaches 980 °C.

2. In the studied range, the rotation frequency of the welding tool has a minor influence on copper temperature in the sites of weld formation.

3. Analysis of thermal cycles at FSW of plates from materials with high heat conductivity at different process parameters of welding suggests two vari-

ants of weld formation. They differ by the nature of the change of metal temperature along the welds at the moment of their formation, depending on speeds of horizontal movement of the welding tool. At tool speeds, which exceed the linear velocity of temperature propagation in the welded product material, the metal temperature during weld formation will remain constant along their entire length. Such a variant of weld formation at FSW of copper plates of 8–12 mm thickness, by preliminary estimates, is possible at speeds of the tool horizontal movement, exceeding 100 mm/min. At tool movement speeds lower than the linear velocity of temperature propagation in the welded product material, the metal temperature at the moment of weld formation will rise with their length. In this case, forced cooling of the welded product should be used, in order to obtain sound welds.

1. Thomas, W.M. (1991) *Friction stir butt welding*. Pat. 9125978.8 GB, Publ. 01.12.91.
2. Dawes, C., Thomas, W. (1995) *TWI Bull.*, **6**, Nov/Dec.
3. Savolainen, K. (2012) *DPh: Friction stir welding of copper and microstructure and properties of the weld*. Aalto University publication series 13/2012.
4. Manish P. Meshram, Basanth Kumar Kodli, Suhash R. (2014) Dey: Friction stir welding of austenitic stainless steel by pcbn tool and its joint analyses. In: *Proc. of 3rd Int. Conf. on Materials Processing and Characterization (ICMPC 2014)*.
5. Brian T. Thompson. (2010) *Thesis: Tool degradation characterization in the friction stir welding of hard metals*. The Ohio State University.
6. De P.S., Kumar N., Mishra R.S. (2005) Fundamentals of Friction Stir Welding. *ASM Handbook*. **6A**, 186–199.
7. Hwang, Y.M., Fan, P.L., Lin, C.H. (2010) Experimental study on friction stir welding of copper metal. *J. Materials Proc. Technology*, **210**, 1667–1672.
8. Pavlova, V.I., Alifirenko, E.A., Osokin, E.P. (2009) Study of temperature-time conditions of welding heating, structure and properties of metal of butt joints from aluminium-magnesium alloy produced by friction stir welding. ISSN 1994-6716. *Voprosy Materialovedeniya*, **4**, 60. St.-Petersburg, TsNII KM Prometey [in Russian].
9. Grigorenko, G.M., Poleshchuk, M.A., Adeeva, L.I. et al. (2016) Peculiarities of structure of Cu-Cu, Ni-Cu and steel-Cu joints produced by overlap friction stir welding method. *The Paton Welding J.*, **5–6**, 75–80.
10. Krasnovsky, K., Khokhlova, Yu.A., Khokhlov, M.A. (2019) Influence of tool shape for friction stir welding on physico-mechanical properties of welded joints of EN AW 6082-T6 aluminium alloy. *Ibid.*, **7**, 9–15 [in Russian].
11. Grigorenko, G.M., Adeeva, L.I., Tunik, A.Yu. et al. (2015) Restoration repair of slab copper moulds of MCCB. Structure and properties of metal in the joint zone. *Sovrem. Elektrometall.*, **1**, 44–49 [in Russian].
12. Grigorenko, G.M., Adeeva, L.I., Tunik, A.Yu. et al. (2014) Structural features of FSW joints of metals with different element solubility in the solid phase. *The Paton Welding J.*, **4**, 13–23.
13. [https://www.bnl.gov/magnets/Staff/Gupta/cryogenic-databook/Section 15.pdf](https://www.bnl.gov/magnets/Staff/Gupta/cryogenic-databook/Section%2015.pdf)

Received 02.02.2021